Cost-Efficient Wearable Blood Glucose Monitoring Through Automated Intravenous Cannula Sampling

Mingyu Zhao[1], Yutong Wang[1], Hen-Wei Huang[1,2]
[1]School of Electrical and Electronic Engineering, Nanyang Technological University, Republic of Singapore
[2]Lee Kong Chian School of Medicine, Nanyang Technological University, Republic of Singapore
Email: mingyu.zhao@ntu.edu.sg

***Abstract*—Frequent blood glucose monitoring is critical for patients receiving insulin therapy and intensive clinical care. Yet, current inpatient workflows rely predominantly on manual blood sampling or disposable sensing components, increasing clinical workload and delaying actionable feedback. Moreover, the overall cost of monitoring scales linearly with the number of tests performed. Although continuous glucose monitoring (CGM) systems offer a cost advantage in that sampling frequency does not directly increase per-use cost, they provide indirect measurements and are not universally suitable for inpatient settings. Existing automated blood analysis platforms also remain constrained by their reliance on single-use sensors or cartridges, which limits scalability and cost efficiency for high-frequency glucose testing in clinical environments. In this work, we present a cost-effective, fully automated point-of-care system for frequent blood glucose monitoring based on intravenous (IV) cannula access. The proposed platform enables automated blood withdrawal, glucose measurement, sensor cleaning, and controlled push-back within a closed microfluidic system, allowing a single glucose sensor to be reused across multiple measurements without contamination or increased consumable cost. A functional prototype has been developed and validated using glucose standard solutions. Over a three-day evaluation period, the system used a single sensor and performed 72 glucose measurements with frequent 2-point calibrations for every 3 hours, showing a 97.2 % confidence interval in +-12% error range. These results indicate the feasibility of a reusable-sensor-based, fully automated IV cannula platform for frequent bedside glucose monitoring, offering a promising solution to reduce clinical workload and per-test cost while enabling high-frequency blood glucose assessment.**

***Index Terms*—Point-of-care testing, blood glucose monitoring, automation, intravenous cannula, reusable sensor, microfluidics**

I. Introduction

Frequent and accurate blood glucose monitoring is essential for a wide range of hospitalized patients, including individuals receiving insulin therapy [1], post-operative patients, and those with unstable glycemic profiles [2]. Rapid fluctuations in blood glucose can occur within short time intervals, particularly in acute care settings, making timely and reliable measurement critical for clinical decision-making [3]. However, existing glucose monitoring workflows in hospitals remain largely manual, intermittent, and resource-intensive [4].

The accuracy of glucose monitoring is fundamentally influenced by the sampling site and the physiological compartment being measured [5]. Many commonly used approaches rely on capillary blood obtained via finger-prick sampling or on interstitial fluid measurements provided by continuous glucose monitoring (CGM) systems. Finger-prick measurements are susceptible to variability arising from sampling technique, residual alcohol from skin preparation [6], and local perfusion conditions. CGM systems, while offering near-continuous readouts, measure glucose in interstitial fluid, which is known to exhibit physiological lag relative to blood glucose and reduced accuracy during rapid glycemic changes [7]–[9]. In contrast, venous blood directly reflects systemic glucose concentration and remains the clinical reference standard for accurate glucose assessment [10]. Enabling automated glucose measurement from venous blood therefore provides a more direct and timely representation of a patient's glycemic status.

Beyond measurement accuracy, current glucose monitoring practices impose a substantial burden on healthcare personnel. Bedside glucose testing typically requires repeated manual blood sampling, handling, and measurement by trained staff,

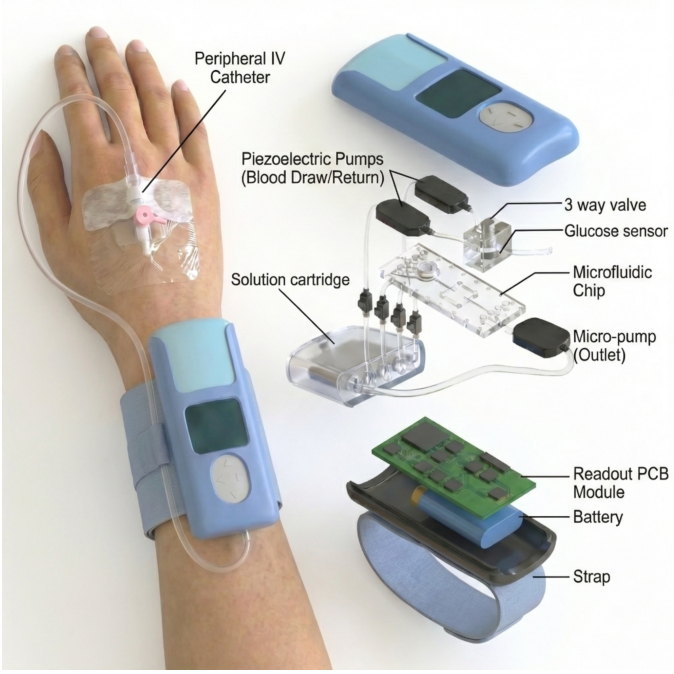

Fig. 1. Conceptual illustration of the proposed automated IV cannula–based blood glucose monitoring system. The graphic was rendered with the assistance of Google Gemini.

This work was supported by A*STAR MedTech MTC Programmatic Seed Grant (M24N9b0130).

introducing procedural variability and increasing the risk of human error. These workflows consume significant clinical resources and inherently limit measurement frequency [11]. An automated system that performs both blood sampling and glucose measurement in a manner analogous to standard clinical practice has the potential to reduce manual workload, minimize operational risk, and support tighter glycemic control through higher-frequency monitoring.

Importantly, the proposed platform is specifically designed for patients who already have a peripheral intravenous cannula (PIVC) in place. PIVCs are routinely inserted for post-operative care, intravenous medication delivery, and fluid management, and are commonly maintained for extended periods in hospitalized patients [12]. This population includes individuals requiring post-surgical glucose control, patients with diabetes mellitus experiencing unstable glycemia, critically ill patients, and those receiving therapies that affect glucose metabolism, such as corticosteroids or parenteral nutrition [13]. Given the size of this patient population and the clinical demand for accurate and frequent glucose monitoring, an automated venous blood–based monitoring system represents an accurate and minimally invasive solution [14].

Another key design objective of the system is to enable repeated use of a single glucose sensor across high-frequency measurements. In conventional point-of-care workflows, sensor consumables scale directly with measurement frequency, resulting in rapidly increasing cost and logistical burden when frequent monitoring is required [15], [16]. By combining reusable glucose sensing with fully automated fluid handling and sensor cleaning, the proposed platform decouples measurement frequency from sensor replacement, thereby avoiding cumulative consumable cost and reducing manual intervention.

In this paper, we present a cost-effective, fully automated point-of-care system for frequent blood glucose monitoring based on venous blood sampling via an intravenous cannula, as shown in the conceptual illustration in Fig. 1. The proposed platform integrates automated blood sampling, glucose measurement, cleaning, calibration, and push-back operations within a closed microfluidic system.

System feasibility is demonstrated through repeated glucose measurements using standard solutions over a continuous 3-day period, corresponding to a typical duration of peripheral IV cannula placement [17], [18]. These results highlight the potential of the proposed approach for high-frequency bedside glucose monitoring in clinical scenarios where frequent blood sampling is required.

The main contributions of this work are:

- A reusable glucose sensing strategy that avoids unaffordable cumulative cost and maintains high sensitivity
- An integrated hardware platform combining custom PCB, microfluidics, pumps, and valves enabling programmable automated measurements
- Validation using standard glucose solution with 72 measurements over three days demonstrating stable and accurate performance

II. System Architecture and Design

A. Overall System Architecture

The proposed system is designed to interface directly with an intravenous cannula, enabling repeated blood access through a single insertion point. The overall architecture consists of four main subsystems: (1) an IV cannula interface and microfluidic network, (2) an automated fluid handling module, (3) a glucose sensing module, and (4) an electronic control and power management unit.

Fig. 2 shows the automation flow schematic. Blood is withdrawn from the IV cannula into a closed microfluidic pathway, transported to a measurement chamber containing the glucose sensor, and subsequently flushed and returned through a controlled push-back mechanism. Cleaning buffers and waste channels are integrated into the disposable fluid pathway to enable automated sensor cleaning and prevent cross-contamination between measurements.

B. Automated Blood Sampling and Push-Back Mechanism

The system employs an automated blood sampling strategy based on coordinated control of micro-pumps and micro-valves with predefined actuation parameters selected according to blood shear rate constraints. This approach enables reliable withdrawal of blood from a peripheral vein through an intravenous cannula while minimizing mechanical stress on blood components [19].

During each measurement cycle, only 500 μL of blood is drawn into a 3D-printed microfluidic channel primed and locked with heparinized saline to prevent clot formation [20]. A dedicated reservoir with a bubble trap temporarily accommodates the withdrawn blood, limiting diffusion into heparinized saline source and preventing air bubbles from entering the patient's vein [21]. A 3/2 solenoid valve by The LEE company (LHDA1211411H) then directs a controlled portion (around 50 μL) of the blood to a parallel glucose sensing module for measurement. Subsequently, a push-back and flushing operation is performed by pumping approximately 1.5 ml of heparinized saline through the fluid pathway with a flow rate of 4.71 ml/min, which is precisely controlled by the piezoelectric pump. This step removes residual blood from the micro channels and re-establishes saline locking, reducing blood stagnation and clotting risk [22]. With this

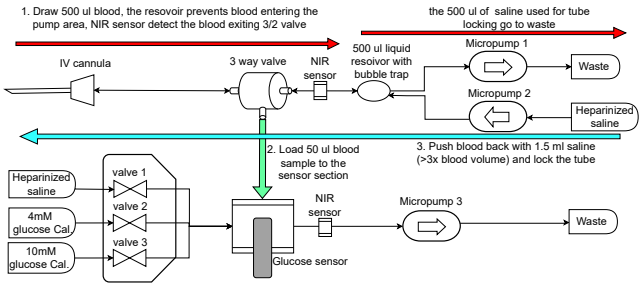

Fig. 2. System architecture of the proposed automated blood glucose monitoring platform.

setup, the blood amount required for measurements is greatly reduced, avoiding the danger of anemia [23]. By separating the blood handling and sensing subsystems, the architecture minimizes sensor contamination and supports robust, long-term automated operation with reduced dead volume and improved cleanliness.

C. Automated glucose measurement, cleaning and calibration

Automated glucose measurement in the proposed system is initiated by a flow-triggered control mechanism based on the spectral sensor modules. Under normal conditions, blood flows through the normally open port of the solenoid valve. When the upstream optical spectral sensor detects the presence of blood, the 3/2 solenoid valve is actuated, redirecting the blood flow into the glucose measurement chamber containing the glucose sensor.

Upon actuation, blood is actively pumped into the sensing chamber and another downstream spectral sensor ensures a sufficient exposure (around 50 μL) of the sensor to fresh blood, while minimizing sample volume and residence time. Following signal acquisition, the glucose measurement is terminated and the system immediately transitions to a cleaning phase. A dedicated washing buffer is automatically pumped through the sensing chamber to remove residual blood components and reduce protein adsorption on the sensor surface.

To support long-term stable operation, two calibration buffers are introduced into the sensing chamber through the same microfluidic pathway. These buffers provide controlled reference conditions for periodic two-point sensor calibration without requiring sensor replacement or manual intervention.

D. Hardware Integration and Control Logic

A custom-designed printed circuit board (PCB) serves as the central control unit of the proposed system, integrating sensing, actuation, power management, and control within a compact hardware platform. The PCB is built around an ESP32-S3 microcontroller unit (MCU), which provides sufficient computational capability, multiple communication interfaces, and real-time control for coordinated system operation.

The fluidic actuation subsystem is driven by three piezoelectric micro-pumps by Bartels Mikrotechnik (BP7) and four micro-solenoid valves, including three active 2/2-way normal-closed valves by MEMETIS (MVL-22-NC-08-14P-PEEK-SIL) and one 3/2-way microvalve by The Lee Company. To support these components, a dedicated four-channel piezo pump driver was designed and implemented on the PCB, enabling independent control of pump frequency and actuation amplitude. Valve control is achieved using ULN2003A driver arrays, providing reliable switching and electrical isolation for solenoid actuation.

A self-designed power management module is integrated on the PCB to support battery-powered operation. A lithium battery serves as the primary power source, and regulated voltage rails of 1.8 V, 3.3 V, 5 V, and 12 V are generated to meet the heterogeneous power requirements of the MCU, sensors, pumps, valves, and analog front-end circuitry. This multi-rail architecture ensures stable operation of all subsystems under varying load conditions.

The glucose measurement subsystem is implemented using a commercial electrochemical glucose sensor (Zimmer & Peacock) interfaced through a custom-designed analog front-end and signal acquisition module. In addition, a modular spectral sensor PCB is integrated into the system to enable closed-loop control of blood detection and flow-triggered actuation. Signals from the spectral sensor are processed by the MCU to initiate valve switching and pump actuation during automated blood sampling.

Control firmware running on the MCU coordinates all system operations, including blood sampling, glucose measurement timing, automated cleaning, calibration buffer delivery, and push-back control. The system logic is fully programmable, allowing measurement frequency, fluid handling parameters, and actuation sequences to be adjusted as required. Tight synchronization between sensing and actuation ensures airtight operation and reproducible fluid behavior, enabling reliable and repeatable automated workflows suitable for high-frequency blood glucose monitoring.

E. Disposable fluid multi-chamber cartridge

The system integrates a disposable multi-chamber fluid cartridge to support automated operation, calibration, and waste handling within a compact and wearable form factor. The bag contains separate reservoirs for heparinized saline, 4 mM and 10 mM glucose calibration buffers, and a waste chamber .

The multi-chamber fluid cartridge bag is planed to be fabricated from polypropylene (PP), wchich is lightweight, disposable, and suitable for medical usage [24]. With a total volume below 50 mL, the bag supports wearable use while maintaining hygienic and fully automated system operation.

III. Experimental Validation

A. Materials for Experiments

All validation experiments were conducted using standard glucose solutions to assess system performance under controlled conditions. A stock D-(+)-glucose solution (100 g/L in H_2O, Merck) was used to prepare glucose standards at concentrations of 4 mM, 6 mM, and 10 mM. Dulbecco's phosphate-buffered saline (PBS, Biowest) was used as the base solution for all dilutions.

To verify the stability and consistency of the prepared glucose standards, the glucose concentration of each solution was measured daily using a commercial glucometer (Accu-Chek Active, Roche) with corresponding test strips. Each standard solution was measured three times, and the average value was recorded as the reference concentration. Only solutions exhibiting stable and consistent readings were used for subsequent automated measurements.

B. Experimental Setup and Automated Measurement Protocol

Experiments were performed using the fully automated blood glucose monitoring system described in the previous sections. The system was programmed to operate in repeated

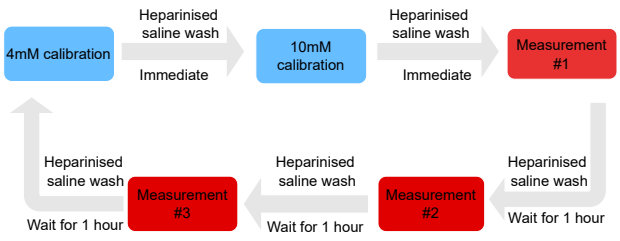

Fig. 3. Flow diagram of the automated measuring process

measurement cycles with a nominal interval of three hours, incorporating automated calibration, cleaning, and glucose measurement steps as shown in Fig.3.

Each cycle began with a two-point calibration using predefined glucose calibration buffers, followed by automated cleaning of the sensing chamber and subsequent glucose measurement. Fluid handling was controlled using integrated micro-pumps and normally closed micro-valves synchronized according to a predefined timing sequence. The piezoelectric micro-pumps were operated at a frequency of 80 Hz with an actuation amplitude of 250, and each pumping action was maintained for 5 s. The corresponding micro-valves were actuated in synchrony with the pump operation to ensure complete fluid replacement between the solution reservoirs and the glucose sensing chamber. Both theoretical analysis and empirical testing confirmed that these parameters were sufficient to fully exchange the fluid volume within the microfluidic pathway.

Automated glucose measurements were performed at one-hour intervals and uniformly distributed across a 24-hour period, enabling high-frequency monitoring without manual intervention. This experimental protocol was designed to emulate frequent bedside glucose testing while maintaining consistent operating conditions throughout the evaluation period.

C. Data Acquisition and Processing

Raw sensor current signals were sampled at 1 Hz and are denoted as

$$I(t_i), \quad i = 1, 2, \ldots, N, \tag{1}$$

where $I(t_i)$ represents the measured current at time t_i and N is the total number of acquired samples.

To ensure that the electrochemical response reached a steady-state plateau after solution exchange, a minimum of $N \geq 40$ samples was collected for each measurement. For $k \geq 20$, a sliding window containing the most recent 20 samples was defined as

$$\mathcal{W}_k = \{I(t_{k-19}), I(t_{k-18}), \ldots, I(t_k)\}. \tag{2}$$

The mean current within this window was calculated as

$$\mu_k = \frac{1}{20} \sum_{j=k-19}^{k} I(t_j), \tag{3}$$

and the corresponding standard deviation was given by

$$\sigma_k = \sqrt{\frac{1}{19} \sum_{j=k-19}^{k} (I(t_j) - \mu_k)^2}. \tag{4}$$

The coefficient of variation (CV) was then defined as

$$\mathrm{CV}_k = \frac{\sigma_k}{\mu_k}. \tag{5}$$

Signal acquisition was terminated when both conditions

$$N \geq 40 \quad \text{and} \quad \mathrm{CV}_k \leq 0.04 \tag{6}$$

were satisfied, indicating sufficient signal convergence.

The final steady-state current value was obtained by averaging the last 20 samples:

$$I_{\text{final}} = \frac{1}{20} \sum_{j=k-19}^{k} I(t_j). \tag{7}$$

For calibration cycles, two reference points (C_1, I_1) and (C_2, I_2) were used to construct a linear calibration model

$$I = aC + b, \tag{8}$$

where the calibration parameters were calculated as

$$a = \frac{I_2 - I_1}{C_2 - C_1}, \qquad b = I_1 - aC_1. \tag{9}$$

For measurement cycles, the glucose concentration $\hat{C}$ was estimated by inverting the calibration model:

$$\hat{C} = \frac{I_{\text{final}} - b}{a}. \tag{10}$$

To ensure measurement consistency, three consecutive concentration estimates $\hat{C}_{n-2}$, $\hat{C}_{n-1}$, and $\hat{C}_n$ were compared. If the deviation satisfied

$$\max(\hat{C}_{n-2}, \hat{C}_{n-1}, \hat{C}_n) - \min(\hat{C}_{n-2}, \hat{C}_{n-1}, \hat{C}_n) > \Delta C_{\max}, \tag{11}$$

the system generated a warning and initiated an additional compensatory measurement.

D. Experimental Results

Fig. 4 shows the time-resolved current response of the glucose sensor during automated operation under stepwise glucose concentration changes. The glucose concentration was sequentially varied between 0 mM, 4 mM, 6 mM, and 10 mM using the automated fluid handling system.

Following each concentration transition, a transient response is observed, corresponding to solution exchange and pressure equilibration during pump and valve actuation. After the transient phase, the sensor signal converges to a stable steady-state plateau at each concentration level. Repeated exposure to the same concentration levels results in comparable steady-state responses, demonstrating reproducible sensor behavior during repeated automated measurement cycles.

These results demonstrate that the proposed automated system supports stable and repeatable glucose sensing under dynamic operating conditions, providing a reliable basis for

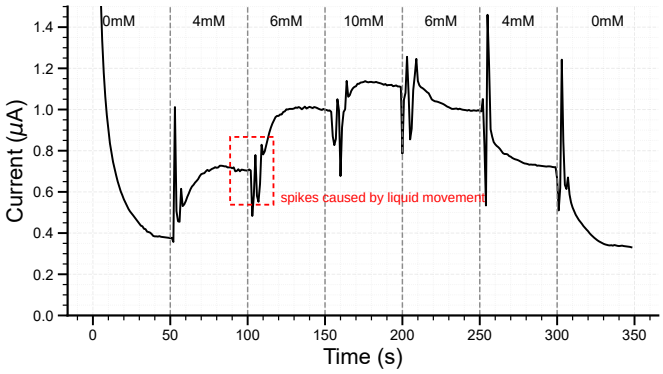

Fig. 4. Dynamic Current Response of a Glucose Sensor Under Stepwise Glucose Concentrations

high-frequency glucose monitoring using automated sampling and fluid switching.

Fig. 5 shows a heatmap representation of sensor current responses and predicted glucose concentrations obtained from a continuous 3-day experiment, collecting total 120 data points (72 measuremnts and 48 calibrations). Each row corresponds to an automated test cycle, while columns represent reference concentrations and its corresponding label. From the heatmap, no clear monotonic trend is observed across the test cycles for all the concentration groups. At the same time, noticeable cycle-to-cycle variations in current levels can be seen, indicating the presence of temporal drift and short-term fluctuations during prolonged automated operation.

Despite these variations, the predicted 6 mM, which is denoted as 6 (pred), responses show a similar temporal pattern to the three measured 6 mM conditions, including the measurements obtained one and two hours after calibration, denoted as 6 (+1h) and 6 (+2h), respectively. The close correspondence between these trends suggests that the two-point linear calibration remains effective in reflecting the changing sensor response over time, allowing the estimated

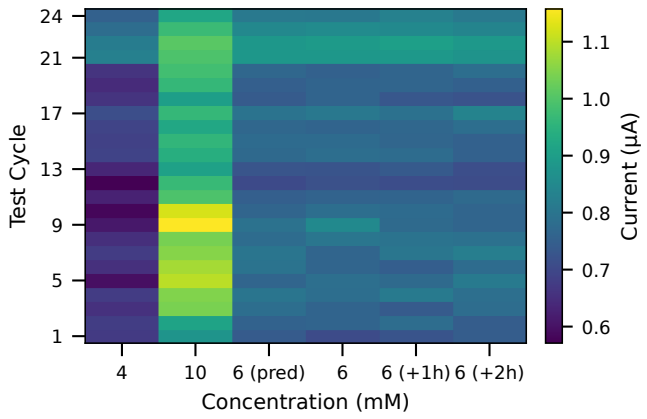

Fig. 5. Time-resolved heatmap of sensor current responses for reference and predicted glucose concentrations during automated operation.

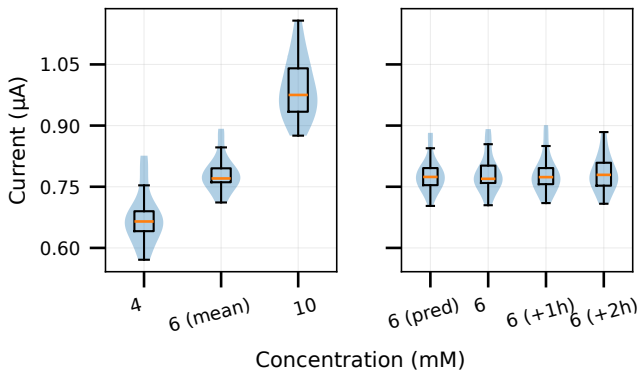

Fig. 6. Distribution of sensor current responses for reference and predicted glucose concentrations across repeated measurements.

concentration to follow the observed drift rather than diverging from the measured values.

Fig. 6 summarizes the distribution of steady-state sensor current responses for the reference glucose concentrations (4 mM and 10 mM) and the corresponding predicted and measured 6 mM conditions across repeated measurements. In the left panel, the current distributions at 4 mM and 10 mM are clearly separated, indicating distinct and concentration-dependent sensor responses that provide effective reference points for two-point calibration.

In the right panel, the distributions of sensor responses for the predicted 6 mM condition and the measured 6 mM values obtained immediately, as well as one and two hours after calibration, show substantial overlap. The median values and spread of these distributions are comparable, indicating that the predicted and measured responses at 6 mM remain consistent over time. Although some variability is observed within each group, no systematic shift in the distribution is apparent with increasing time after calibration.

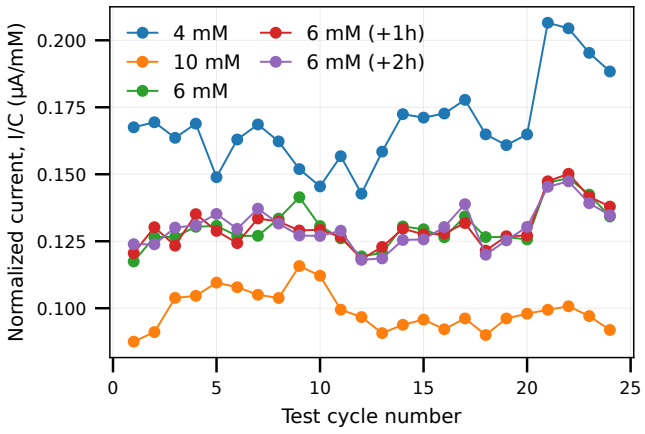

Fig. 7. Concentration-normalized sensor response (I/C) versus test cycle number (4–10 mM with repeated 6 mM checks)

Together, these results suggest that while the sensor exhibits

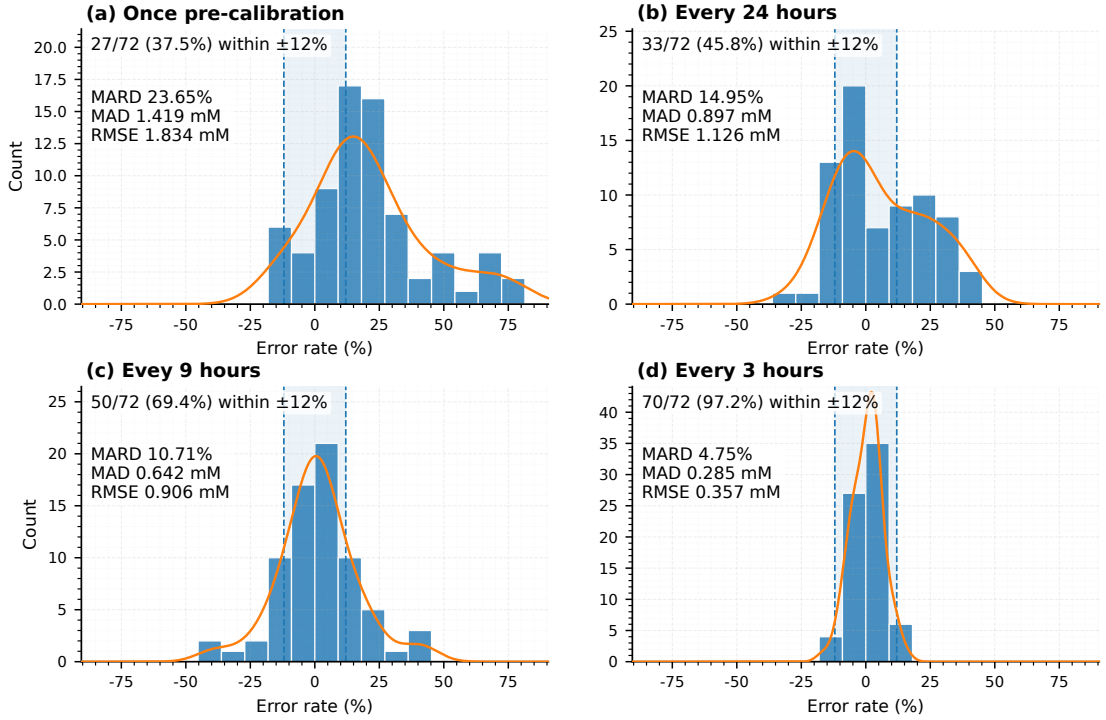

Fig. 8. Percentage error rate of the glucose sensor over 72 times over 3 days with different calibration frequencies:(a) Only once 2-point calibration in the beginning; (b) 2-point calibration at the beginning of every 24 hours; (c) 2-point calibration for every 9 hours; (d) 2-point calibration for every 3 hours;

inherent measurement variability, the two-point calibration approach yields concentration estimates that are consistent with the measured sensor response at 6 mM over repeated measurement cycles. The maintained separation between reference concentrations and the overlapping distributions at 6 mM support the validity of the calibration and signal processing strategy under extended automated operation.

Fig. 7 shows the concentration-normalized sensor response (I/C) as a function of test cycle number for glucose concentrations of 4 mM, 6 mM, and 10 mM. By normalizing the measured current by concentration, this representation highlights changes in the effective sensor response that are independent of absolute glucose level.

Across the test cycles, the normalized responses exhibit noticeable cycle-to-cycle variation, indicating the presence of temporal drift and short-term fluctuations during extended automated operation. No clear monotonic trend is observed for any concentration, suggesting that the response changes are not dominated by a single unidirectional degradation process.

Importantly, the normalized responses corresponding to the repeated 6 mM measurements, including those acquired one and two hours after calibration, closely follow the same temporal pattern as the primary 6 mM measurements. This agreement indicates that the relative response to concentration is preserved over successive cycles, despite variations in the absolute sensor output. In contrast, the 4 mM and 10 mM responses remain clearly separated from the 6 mM group, demonstrating maintained concentration-dependent differentiation.

Together, these observations suggest that while the enzyme-based sensor exhibits temporal variability during prolonged operation, the proportional relationship between sensor current and glucose concentration remains consistent. This behavior supports the use of periodic calibration and concentration-based normalization to compensate for drift and enables reliable comparison of measurements across repeated automated test cycles.

To further evaluate the impact of calibration strategy on system performance, Fig. 8 compares the percentage error distributions obtained under different calibration frequencies using the same 72-measurement dataset. Four calibration schemes were evaluated: a single global two-point calibration, calibration every 24 measurements, every 9 measurements, and every 3 measurements. Error metrics including mean absolute relative difference (MARD), mean absolute deviation (MAD), and root mean square error (RMSE) were computed for each case.

As shown in Fig. 8(a), using a single global calibration results in substantial error dispersion and limited agreement within a ±12% error range, which is the FDA standard for point-of-care glucose monitoring device [25]. Increasing the calibration frequency progressively reduces both the spread and magnitude of measurement errors, as reflected by improvements in MARD, MAD, and RMSE in Fig. 8(b) and Fig. 8(c). The best performance is achieved when a two-point calibration is performed every three measurements, as shown in Fig. 8(d), where 97.2% of the measurements fall within ±12% error and the error distribution becomes tightly centered.

These results demonstrate that frequent, automated calibration effectively compensates for short-term sensor variability and system-level drift during extended operation. Based on this analysis, the calibration frequency of one two-point calibration every three measurements was selected as a practical balance between measurement accuracy and operational efficiency for the proposed system.

IV. Conclusion

This work presents a cost-efficient, fully automated point-of-care system for frequent blood glucose monitoring via intravenous cannula access. By integrating automated fluid handling, reusable glucose sensing, and programmable control within a microfluidic platform, the system enables repeated blood glucose measurements without increasing per-test consumable cost. Experimental validation using standard glucose solution demonstrates stable and accurate performance over 72 automated measurements across three days, highlighting the feasibility of the proposed approach for high-frequency bedside glucose monitoring.

References

[1] M.-C. Zanella, G. Catho, H. Jackson, N. Lotfinejad, V. Sauvan, M.-N. Chraiti, W. Zingg, S. Harbarth, and N. Buetti, "Dwell time and risk of bloodstream infection with peripheral intravenous catheters," *JAMA Netw. Open*, vol. 8, no. 4, e257202, Apr. 2025, doi: 10.1001/jamanetworkopen.2025.7202.

[2] B. Hagerf *et al*., "Accuracy and feasibility of real-time continuous glucose monitoring in critically ill patients after abdominal surgery and solid organ transplantation," *Diabetes Care*, vol. 47, pp. 956–963, 2024, doi: 10.2337/dc23-1663.

[3] B. Kovatchev and C. Cobelli, "Glucose variability: Timing, risk analysis, and relationship to hypoglycemia in diabetes," *Diabetes Care*, vol. 39, pp. 502–510, 2016, doi: 10.2337/dc15-2035.

[4] N. K. Tran, C. LaValley, B. Bagley, and J. Rodrigo, "Point of care blood glucose devices in the hospital setting," Crit. Rev. Clin. Lab. Sci., vol. 60, no. 4, pp. 290–299, Jun. 2023, doi: 10.1080/10408363.2023.2170316.

[5] G.-J. Eerdekens, S. Rex, and D. Mesotten, "Accuracy of blood glucose measurement and blood glucose targets," J. Diabetes Sci. Technol., vol. 14, no. 3, pp. 553–559, May 2020, doi: 10.1177/1932296820905581.

[6] Critchell, D., Savarese, V., Callahan, A., Aboud, C., Jabbour, S., and Marik, P. (2006). Accuracy of bedside capillary blood glucose measurements in critically ill patients. Intensive Care Medicine, 33, 2079-2084. https://doi.org/10.1007/s00134-007-0835-4.

[7] K. M. Hutchins, J. A. Betts, D. Thompson, A. Hengist, and J. T. Gonzalez, "Continuous glucose monitor overestimates glycemia, with the magnitude of bias varying by postprandial test and individual – a randomized crossover trial," Am. J. Clin. Nutr., vol. 121, no. 5, pp. 1025–1034, May 2025, doi: 10.1016/j.ajcnut.2025.02.024.

[8] W. V. Gonzales et al., "The progress of glucose monitoring—A review of invasive to minimally and non-invasive techniques, devices and sensors," Sensors, vol. 19, no. 4, p. 800, 2019, doi: 10.3390/s19040800.

[9] A. Heller and B. Feldman, "Electrochemical glucose sensors and their applications in diabetes management," Chemical Reviews, vol. 108, no. 7, pp. 2482–2505, 2008, doi: 10.1021/cr068069y.

[10] K. Macleod, L. B. Katz, and H. Cameron, "Capillary and venous blood glucose accuracy in blood glucose meters versus reference standards: The impact of study design on accuracy evaluations," *J. Diabetes Sci. Technol.*, vol. 13, no. 3, pp. 546–552, May 2019, doi: 10.1177/1932296818790228.

[11] D. Aragon, "Evaluation of nursing work effort and perceptions about blood glucose testing in tight glycemic control," Am. J. Crit. Care, vol. 15, no. 4, pp. 370–377, Jul. 2006, doi: 10.4037/ajcc2006.15.4.370.

[12] S. Berger, K. Winchester, R. B. Principe, and E. Culverwell, "Prevalence of peripheral intravenous catheters and policy adherence: A point prevalence in a tertiary care university hospital," J. Clin. Nurs., vol. 31, no. 15–16, pp. 2324–2330, Aug. 2022, doi: 10.1111/jocn.16051.

[13] E. Alexandrou et al., "Use of short peripheral intravenous catheters: characteristics, management, and outcomes worldwide," J. Hosp. Med., vol. 13, no. 5, pp. E1–E7, May 2018, doi: 10.12788/jhm.3039.

[14] D. Hochfellner et al., "Accuracy and safety of a novel intravenous continuous glucose monitoring system in patients admitted to a cardiothoracic ICU: A pilot trial," J. Diabetes Sci. Technol., early access, May 24, 2025, Art. no. 19322968251342598, doi: 10.1177/19322968251342598.

[15] I. Oyagüez, J. Merino-Torres, M. Brito, V. Bellido, R. Cardona-Hernández, F. Gómez-Peralta, and F. Morales-Pérez, "Cost analysis of the flash monitoring system (FreeStyle Libre 2) in adults with type 1 diabetes mellitus," *BMJ Open Diabetes Res. Care*, vol. 8, e001330, 2020, doi: 10.1136/bmjdrc-2020-001330.

[16] I. Oyagüez, J. Merino-Torres, M. Brito, V. Bellido, R. Cardona-Hernández, F. Gómez-Peralta, and F. Morales-Pérez, "Cost analysis of the flash monitoring system (FreeStyle Libre 2) in adults with type 1 diabetes mellitus," *BMJ Open Diabetes Res. Care*, vol. 8, e001330, 2020, doi: 10.1136/bmjdrc-2020-001330.

[17] Tripathi, S., and T. Gladfelter, "Peripheral intravenous catheters in hospitalized patients: Practice, dwell times, and factors impacting the dwell times: A single center retrospective study," *The Journal of Vascular Access*, vol. 23, pp. 581–588, 2021, doi: 10.1177/11297298211000874.

[18] M.-C. Zanella, G. Catho, H. Jackson, N. Lotfinejad, V. Sauvan, M.-N. Chraiti, W. Zingg, S. Harbarth, and N. Buetti, "Dwell time and risk of bloodstream infection with peripheral intravenous catheters," *JAMA Netw. Open*, vol. 8, no. 4, e257202, Apr. 2025, doi: 10.1001/jamanetworkopen.2025.7202.

[19] A. W. Browne and C. H. Ahn, "An in-line microfluidic blood sampling interface between patients and saline infusion systems," Biomedical Microdevices, vol. 13, no. 4, pp. 661–669, Aug. 2011, doi: 10.1007/s10544-011-9536-4.

[20] L. F. Harris and A. J. Killard, "Heparin monitoring: From blood tube to microfluidic device," in Heparin: Properties, Uses and Side Effects, D. E. Piyathilake and R. Liang, Eds. Hauppauge, NY, USA: Nova Science Publishers, 2012, ch. 4, pp. 83–108, ISBN: 978-1-62100-431-8.

[21] Y. S. Zhang, S. Chae, A. Polini, M. R. Dokmeci, and A. Khademhosseini, "A highly efficient bubble trap for continuous removal of gas bubbles from microfluidic devices," in Proc. 18th Int. Conf. Miniaturized Syst. Chem. Life Sci. (MicroTAS), San Antonio, TX, USA, Oct. 26–30, 2014, pp. 730–732.

[22] R. Wang et al., "Heparin saline versus normal saline for flushing and locking peripheral venous catheters in decompensated liver cirrhosis patients: A randomized controlled trial," Medicine (Baltimore), vol. 94, no. 31, p. e1292, Aug. 2015, doi: 10.1097/MD.0000000000001292.

[23] T. François et al., "Impact of blood sampling on anemia in the PICU: A prospective cohort study," Pediatric Critical Care Medicine, vol. 23, no. 6, pp. 435–443, Jun. 2022, doi: 10.1097/PCC.0000000000002947.

[24] G. Wypych, "Polypropylene in medical applications," in Handbook of Polymers, 2nd ed. Oxford, U.K.: Elsevier, 2016, pp. 569–572.

[25] U.S. Food and Drug Administration, "Blood Glucose Monitoring Test Systems for Prescription Point-of-Care Use: Guidance for Industry and Food and Drug Administration Staff," Guidance document, Docket No. FDA-2013-D-1445, Document No. 1755, Oct. 11, 2016.